



Article

Environmental and Health Risk Assessment of Soil Adjacent to a Self-Burning Waste Pile from an Abandoned Coal Mine in Northern Portugal

Patrícia Santos ^{1,2,*} , Joana Ribeiro ^{3,4} , Jorge Espinha Marques ^{1,2} and Deolinda Flores ^{1,2}

¹ Institute of Earth Sciences, Pole of University of Porto, 4169-007 Porto, Portugal

² Department of Geosciences, Environment and Spatial Planning FCUP, University of Porto, 4169-007 Porto, Portugal

³ Department of Earth Sciences, University of Coimbra, 3030-790 Coimbra, Portugal

⁴ Instituto Dom Luís (IDL), Faculty of Sciences, University of Lisbon, 1749-016 Lisboa, Portugal

* Correspondence: patricia.santos@fc.up.pt

Abstract: Abandoned mines and disposal of mining residues can be responsible for the release of potentially toxic elements (PTEs) into the environment causing soil and water contamination, with potential ecological damage and human health hazards. The quantification of the apportionment of PTEs in soils and the study of the associated ecological and human health risks are essential. This study aims to assess the environmental and human health risk of the soils surrounding an abandoned coal mine in São Pedro da Cova, whose waste pile has been affected by self-combustion for over 17 years. The soil environmental characterization of the study area regarding PTEs was accessed by different pollution indices, considering the elementary crustal abundance and the determined regional soil geochemical background. The soil contamination degree was evaluated using indices such as the contamination factor (C_f) and geoaccumulation index (I_{geo}), inferred for all soil samples, and the potential ecological risk index (PERI) was also accessed. The human health risk was evaluated for adults and children, considering the non-carcinogenic and carcinogenic risks. The pollution indices calculated for the PTEs using distinct reference values showed significant differences, resulting in lower pollution indices when using the regional reference values. The regional background proved to be a much more reliable geochemical baseline for environmental assessment. Regarding I_{geo} , the soils were found to be unpolluted to moderately polluted for most of the studied PTEs. The determined PERI for the soils surrounding the abandoned mine classifies them as low ecological risk. The evaluation of the non-carcinogenic and carcinogenic risks, resulting from exposure to the studied soils, suggests that there is no potential human health risk for children or adults regarding the considered PTEs.



Citation: Santos, P.; Ribeiro, J.; Espinha Marques, J.; Flores, D. Environmental and Health Risk Assessment of Soil Adjacent to a Self-Burning Waste Pile from an Abandoned Coal Mine in Northern Portugal. *Environments* **2023**, *10*, 53. <https://doi.org/10.3390/environments10030053>

Academic Editor: Manuel Duarte Pinheiro

Received: 31 January 2023

Revised: 9 March 2023

Accepted: 10 March 2023

Published: 13 March 2023



Copyright: © 2023 by the authors. Licensee MDPI, Basel, Switzerland. This article is an open access article distributed under the terms and conditions of the Creative Commons Attribution (CC BY) license (<https://creativecommons.org/licenses/by/4.0/>).

Keywords: pollution; soil; coal; mine; background; combustion; I_{geo} ; PERI; health

1. Introduction

Coal mining, along with disposing coal combustion remains, can concentrate and release to the surrounding soils and waters high concentrations of potentially toxic elements (PTEs), contributing to its ecological degradation [1–3]. Soil pollution with PTEs may increase the risk of its bioaccumulation in the human body through ingestion, dermal absorption, and inhalation [4,5]. Industrial mining activity has been described as a significant source of heavy metals to the surrounding environment [6,7]. The mining infrastructures and waste piles remain for many years following mine closure and abandonment, extending the environmental passive trough time. These mining residues concentrate different PTEs [8,9] that can migrate to the surrounding soils and water systems.

Potentially toxic elements, commonly present in coals [10] and consequently in coal mining residues, can be considered environmentally hazardous, possibly causing human

health problems [11,12]. The percolation and leaching of PTEs from coals and coal mining wastes impact surrounding areas and, besides the atmospheric dispersion of particles, coal-related fires are also a significant source of atmospheric pollutants [9,13].

Soil environmental characterization and risk assessment are typically used to describe soil quality. The use of geochemical pollution indexes can be a very expedite tool to evaluate the degree of soil contamination and they have been widely used worldwide [14,15], being also applied in mining contexts [16–18]. In Portugal these indexes have been applied to soils and sediments to assess contamination surrounding mining areas, such as, e.g., Aljustrel [19], Regoufe [20], Panasqueira [21,22] and different uranium mines [23].

Kowalska et al. [24] conducted a review comparing 18 different indices of pollution, and concluded that among the individual pollution indices, the geoaccumulation index (Igeo) [25] and enrichment factor (EF) [26] were considered the most useful and universal, while the complex pollution indices believed as the most important were potential ecological risk index (PERI) [27] and contamination severity index (CSI) [28]. Generally, these pollution indexes compare elemental concentrations in soils and sediments with a reference value or national criterion for that element or local background [15,18,29]. Soil enrichment in PTEs is often caused by anthropogenic influence; therefore, a comparison of the measured elemental concentrations with a reference that was not influenced by any external source of contamination is critical.

Soil environment background values are the concentrations of elements or components naturally present in the soil that were not affected by anthropogenic activities [30]. The concept of geochemical background aims to distinguish the normal and abnormal concentrations of elements. Trace elements are present naturally in rocks and are transferred into the regional soils according to pedogenetic processes and environmental conditions [31]. They reflect regional geology; however, the trace elements in soils may also be affected by anthropogenic factors and the local land use. Thereby, an abnormal concentration may result from different causes. In the exploration geochemistry field, an abnormal concentration may be an indicator of an ore occurrence, while for environmental geochemistry, it may be an indicator of contamination issues [32,33]. Near mining areas are thereby crucial for the characterization of the regional geochemical background, since they can help to establish threshold values for contamination, allowing to distinguish between the natural concentration of elements present in soils and the areas potentially enriched in determined elements as a result of anthropogenic contamination.

The abandoned mine of São Pedro da Cova is located in Gondomar, northwest of Portugal. It was one of the most significant mines exploited along the Douro Carboniferous Basin. It exploited anthracite A coal [34] for nearly two centuries and closed in 1972 without any rehabilitation until now. In the abandoned mining complex, it is possible to identify old and degraded mining facilities, as well as a waste pile, covering an area of over 28,000 m², rich in carbonaceous residues. In 2005, after ignition caused by wildfires, the southern part of the waste pile started burning and has been self-combusting until the present. The characterization of the mining residues deposited in this waste pile materials, as well as the identification of resultant combustion products, was previously studied, the geochemical composition, petrography and mineralogy of the materials deposited in the waste pile were characterized [35,36], as well as the main organic pollutants [37]. The magnetic susceptibility of the materials deposited in the waste pile, as well as the mineralogical changes due to combustion, were also assessed [38]. Previous studies conducted in this area also investigated the leaching potential and mobility of hazardous elements from the residues deposited in the waste pile [39] and its acid production potential [40]. Since 2018, different studies have been conducted regarding mine environmental monitoring, focusing on the waste pile and the underground mine effluent discharge areas [41]. The geochemistry, mineralogy, and hydrological of the self-burning waste pile were studied from a hydro-pedological perspective [42]. The mining effluents were studied and their physicochemical properties and suitability for irrigation purposes were assessed [43]. The soils surrounding the mine were characterized geochemically for major and trace

elements, and 16 priority polycyclic aromatic hydrocarbons (PAHs) were identified and quantified [44].

The São Pedro da Cova is a densely populated village, developed along the immediate vicinity of the abandoned mining complex, with locals developing small areas of subsistence farming close to the mine. Therefore, the study of the environmental impact caused by past mining activities and facilities on the surrounding soils and its reflection on the ecosystems and human health is imperative. This characterization should provide a valuable tool concerning decision making regarding the requalification and rehabilitation of these degraded areas. In Poland and the Czech Republic, coal fires and coal mining dumps affected by combustion have been studied and environmentally monitored [25,26]. Studies have been conducted regarding the potential reutilization of these abandoned areas [27], concluding that it is possible, with close monitoring, to implement industrial investments in post-mining areas hosting coal waste dumps. Possible land use utilizations could be construction, conversion of the areas for recreational and sports purposes, or the use of the mining residues as secondary raw materials [26].

The aim of this research is to characterize the environmental pollution and risks associated with the soils around the abandoned São Pedro da Cova coal mine. The importance of this study is to provide insight on the risks that population and environment are subjected in this mining area, providing guidance for future decision making regarding rehabilitation and future land use of the area.

The soil quality from fifty samples surrounding the mining facilities and waste pile was assessed, regarding ten selected PTEs. The elemental concentrations were compared with Portuguese reference values, as the crustal elemental distribution and regional background were used to calculate different pollution indices, such as contamination factor (C_f), geoaccumulation index (Igeo), and potential ecological risk index (PERI). This study also intends to contribute to the characterization of the human health risk associated with these soils; therefore, the non-carcinogenic and carcinogenic risks posed to humans were also determined by applying the United States Environmental Protection Agency (USEPA) health risk assessment model.

2. Materials and Methods

2.1. Study Area and Sampling

The mine of São Pedro da Cova (41°09'25" N; 8°30'06" W) is one of the multiple coalfields deposits, hosted in the Douro Carboniferous Basin (DCB), which hosted mineable Upper Pennsylvanian coal seams [45,46]. The DCB has an NW–SE alignment, extending from São Pedro de Fins until Janarde (approximately 53 km in length), with a variable width (30–250 m) [47]. These deposits were generated along structured shear bands, on the late to post-orogenic phases of the Variscan orogeny, and are contiguous to a large geological structure, the Valongo Anticline. This structure extends over 90 km and is oriented according to the NW–SE, corresponding to an antiform fold, formed at the first deformation phase of orogeny (D1), with Paleozoic metasedimentary sequence, in which the oldest rocks are in the nucleus and whose flanks are asymmetric [48]. The studied area is located along the border of the western flank of the structure, where the metasedimentary formations dated from Cambrian to Carboniferous.

A total of fifty soil samples were collected along a 100 m spacing grid, covering an area of about 480,000 m². This regular sampling excluded the coal mine waste pile since these had been the subject of previous studies [35,37,38]. The size and orientation of the grid, preferentially NE–SW was planned to characterize the main drainage basin, located southwest of the mining residues, and according to the dominant wind direction known for the region (from SW towards NE). The sampling sites covered nearly all land uses available in the vicinity of the old mine, including forest, urban and farmed areas, and small landfills (Figure 1).

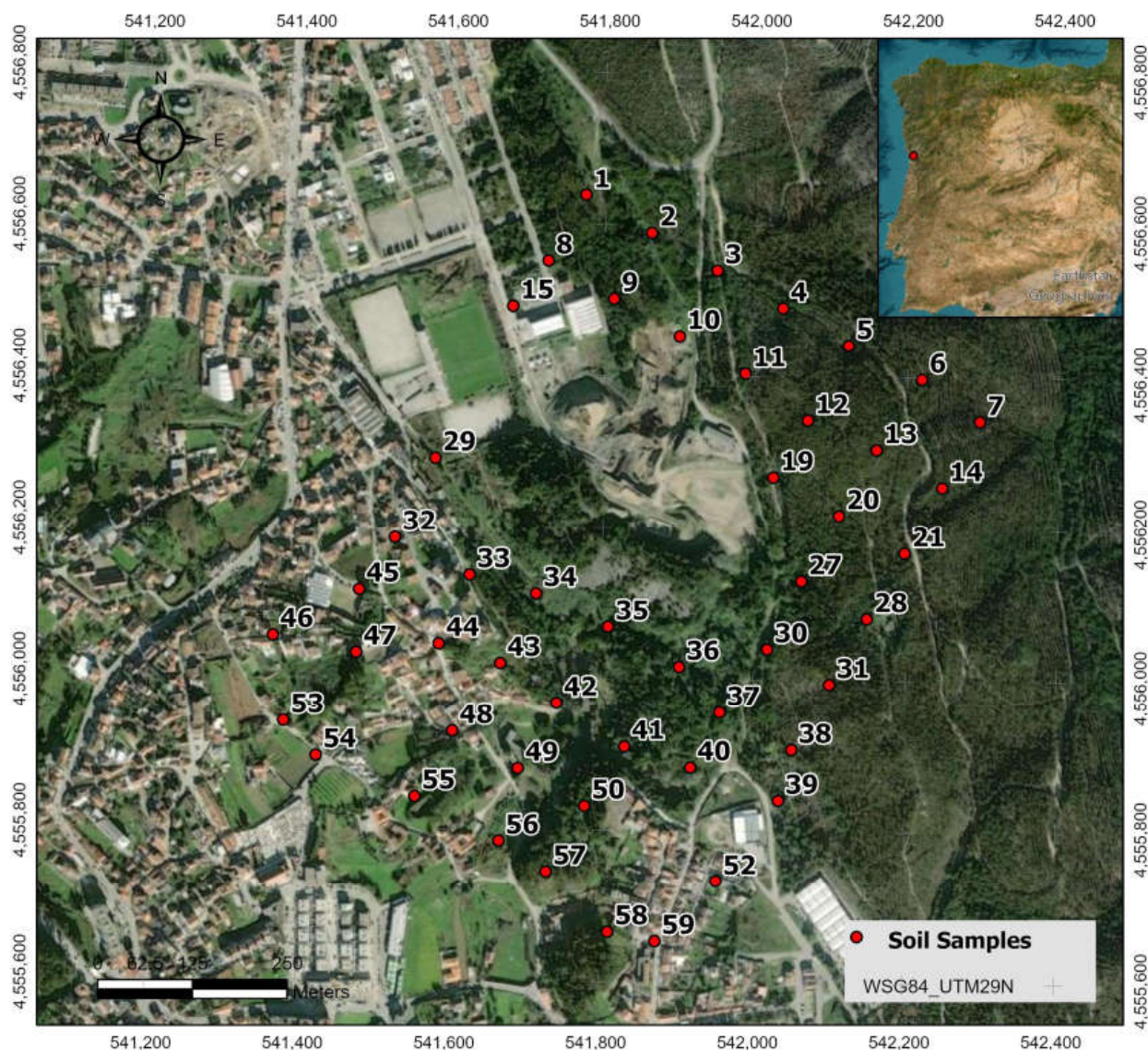


Figure 1. Soil sampling general setting.

Each sample was collected close to the surface (0–20 cm) using a stainless-steel shovel and contained approximately 1.5 kg of soil. The sampling locations were identified using a global positioning system (GPS). Soil samples were dried at room temperature and sieved at 2 mm to remove gravel and organic residues. The samples were quartered to obtain representative samples and then crushed to obtain fractions lower than 80 mesh.

The geochemical composition was determined in the Bureau Veritas Laboratories (Vancouver), by inductively coupled plasma emission spectrometry/mass spectrometry (ICP-ES/MS), after digestion with a multi-acid solution of HF-HClO₄-HNO₃. The QA/QC protocol was insured using analytical results of certified reference materials (STD OREAS25A-4A and STD OREAS45E), blanks, and random duplicate samples. The results were within the 95% confidence limits of the recommended values given for the certified materials. The general geochemical characterization of these soils was already published [44].

2.2. Environmental Pollution Level Assessment

In this research, the assessment of the environmental pollution in the soils surrounding the abandoned mine of São Pedro da Cova was inferred from soil geochemical sampling. The elemental concentrations for 10 PTEs were compared with Portuguese reference values for contaminated soil for agriculture [49], and considering the insertion of this area of study in a large mining district, effort was made to determine the regional background, from preexisting geochemical soil data. Pollution indices, such as C_f and I_{geo} , were determined using as a geochemical baseline the elemental average crustal distribution [50] and the regional geochemical background determined for the study area, to understand the impact of the use of worldwide reference values in pollution studies surrounding mining areas, instead of the local background values. The average I_{geo} values were also determined in subgroups according to the land use of each sample location, based in regional geochemical background, to individualize the results influenced by waste pile leaching and the ones that could potentially result from urban contamination. Similar to I_{geo} , PERI was also determined, following two approaches: using as reference values the crustal concentration of each element and considering the determined regional background.

2.2.1. Regional Geochemical Background Characterization

The regional geochemical background was determined, using a selection of individual geochemical results from samples obtained in two previous soil sampling campaigns performed in 2015 and 2016, during regional soil campaigns for gold exploration [51,52]. These campaigns had covered a significant area of the Valongo Anticline, so they provided valuable information about the geochemical baseline of the area of interest. In order to obtain representative background results of this area, 41 samples were selected from the total database provided, distributed along the western flank of this anticline, covering identical bedrock, in the same geologic units as the present studied area, and hosting similar structures. These samples were selected from four lines, located NW and SE of the studied area, away from possible contamination sources. Three of the lines present a spacing of 2 km between lines, the fourth line shares the same alignment but is positioned 4 km to NW, and the sample spacing is 100 m, crossing the main lithological contacts and regional structures sub-perpendicularly (Figure 2). During the regional survey, the geochemical composition of trace elements had been determined in ASL Laboratories in Seville (Accredited by ISO 17025:2005; INAB registration 173T) by inductively coupled plasma–atomic emission spectroscopy (ICP-AES). Samples were dried below 60 °C, sieved at 2 mm, and pulverized at 75 µm. For each sample, an aliquot of 0.50 g was digested in aqua regia HNO_3 -HCl for 45 min in a graphite heating block. After cooling the resulting solution was diluted in 12.5 mL with deionized water, mixed, and analyzed by ICP-AES. The quality control protocol was insured, certified reference materials (GEO MS-03; ICP-4; OGGGEO08), blanks, and random duplicate samples were analyzed, and the respective results were within the 95% confidence limits of the recommended values given for the certified materials.

Different methods have been used to establish background concentrations of trace metals in soils, including 95th percentile, the means, and upper confidence limit [53–55]. In this study, the background values were calculated from the mean concentrations of heavy metals and metalloids using the geochemical data from 41 selected soil samples [51,52] based on spatial and geological criteria. The use of mean values was preferred as it would represent a more conservative approach, that higher percentiles for environmental assessment. The means were determined after outlier removal, following the approach made by several authors [17,56,57].

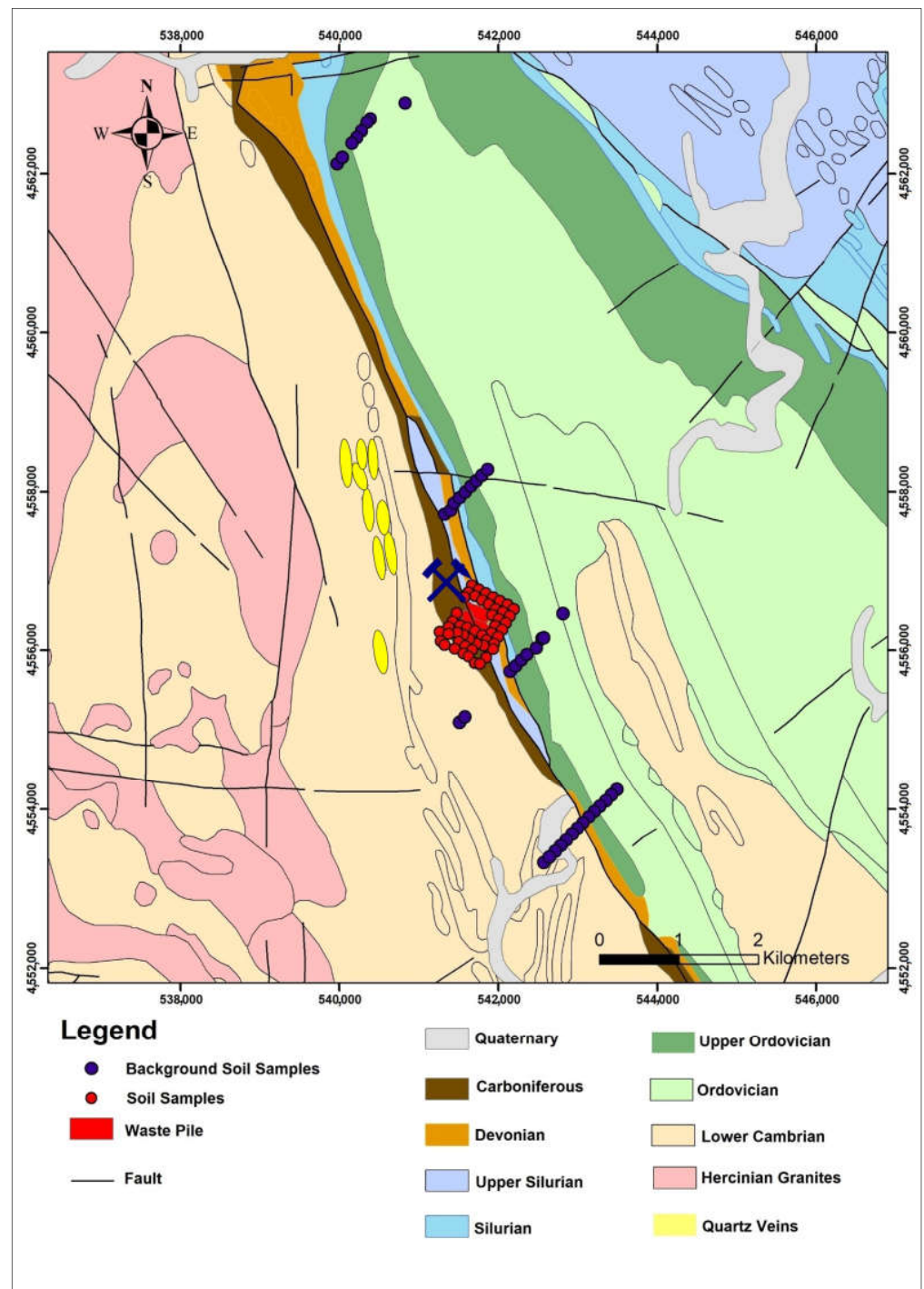


Figure 2. General geologic setting of the studied area with location of soil samples surrounding the waste pile and the samples used to infer the regional geochemical background. Geology adapted from the geological map of Portugal, at scale 1:200,000 [58].

2.2.2. Geoaccumulation Index (Igeo)

The Igeo has been generally used as a reference for estimating the enrichment and pollution level of metals in sediments and soils [17,59–61]. The Igeo can be calculated by the following formula [25]:

$$I_{geo} = \log_2(C_n/1.5B_n) \quad (1)$$

where C_n is the measured heavy metal concentrations in soil, and B_n is the geochemical background concentration of the corresponding element. The constant 1.5 is introduced to minimize the lithospheric effects in the background matrix.

The I_{geo} consists of seven grades or classes and is given as $I_{geo} \leq 0$ unpolluted; $0 < I_{geo} < 1$ unpolluted to moderately polluted; $1 < I_{geo} < 2$ moderately polluted; $2 < I_{geo} < 3$ moderately to heavily polluted; $3 < I_{geo} < 4$ heavily polluted; $4 < I_{geo} < 5$ heavily to extremely polluted; and $I_{geo} > 5$ extremely polluted.

2.2.3. Potential Ecological Risk Index (PERI)

The potential ecological risk in soils surrounding the coal mine was determined using the E_r and risk index (RI) developed by Hakanson [27] and calculated using the following equations:

$$E_r^i = T_r^i \times C_f^i \quad (2)$$

$$C_f^i = C_{iD} / C_{iB} \quad (3)$$

$$RI = \sum_{i=1}^n E_r^i \quad (4)$$

where n is the number of metal(loids), E_r^i is the ecological risk index, and T_r^i is the toxicity coefficient of trace metal i .

The toxicity coefficients of Pb, Zn, Ni, Cu, Cr, Cd, Mn, and As correspond to 5, 1, 5, 5, 3, 30, 1, and 10, respectively [27]. The Sb toxicity coefficient used is 7, according to Wang [59], who calculated the Sb toxicity coefficient based on Hakanson's principles. The C_f^i corresponds to the contamination factor of each heavy metal/metalloid and C_{iD} and C_{iB} correspond to the measured concentration and background value of trace metal i , respectively. The C_f can be interpreted as an individual pollution index, as given: $C_f < 1$ low contamination; $1 < C_f < 3$ moderate contamination, $3 < C_f < 6$ high contamination; $C_f > 6$ very high.

RI is the risk index, meaning the cumulative value of all the E_r^i values of multiple trace metals and metalloids. The potential ecological risk for every single element, E_r^i is given as $E_r^i < 40$ low risk; $40 \leq E_r^i < 80$ moderate risk; $80 \leq E_r^i < 160$ considerable risk; $160 \leq E_r^i < 320$ high risk. RI can be classified into the following classes: $RI < 150$ low risk; $150 \leq RI < 300$ moderate risk; $300 \leq RI < 600$ considerable risk; $RI \geq 600$ high risk.

The spatial distribution of the individual RI determined from the geochemical results of each soil sample was modelled using geostatistical algorithms, namely ordinary kriging, using the Geostatistical Analyst tools, from ESRI ArcGIS PRO [62] software.

2.3. Human Health Risk Assessment Index

Regarding human exposure to heavy metals and metalloids, there are generally three main pathways for exposure: ingestion, inhalation, and dermal contact. In this study, to determine the exposure risks of soil PTEs to the locals, the main exposure types were considered according to the methodology developed by the United States Environmental Protection Agency (USEPA) for health risk assessment [63,64]. The predicted average daily dose (mg element kg^{-1} bodyweight day^{-1}) received through ingestion, inhalation and dermal absorption was calculated according to [65–67] the following equations:

$$D_{ing} = \frac{C \times \text{IngR} \times \text{EF} \times \text{ED}}{\text{BW} \times \text{AT}} \times 10^{-6} \quad (5)$$

$$D_{inhR} = \frac{C \times \text{InhR} \times \text{EF} \times \text{ED}}{\text{PEF} \times \text{BW} \times \text{AT}} \quad (6)$$

$$D_{\text{dermal}} = \frac{C \times SL \times SA \times ABS \times EF \times ED}{BW \times AT} \quad (7)$$

where C stands for the metal or metalloid concentration in soil (mg kg^{-1}); Ingestion rate (children: 200 mg d^{-1} , adults: 100 mg d^{-1}); InhR represents inhalation rate (children: $7.63 \text{ m}^3 \text{ d}^{-1}$; adults: $20 \text{ m}^3 \text{ d}^{-1}$); EF is the exposure frequency (180 d y^{-1}); ED represents the exposure duration (6 years for children and 24 years for adults); BW is the body weight of exposed individual (children: 15 kg; adults: 70 kg); AT is the time period over which the dose was averaged (non-carcinogens: $ED \times 365 \text{ d}$; carcinogens: $70 \times 365 = 25,550 \text{ d}$); PEF is the emission factor ($1.36 \times 10^{-9} \text{ m}^3 \text{ kg}^{-1}$); SL is skin adherence factor (children: $0.2 \text{ mg cm}^{-2} \text{ d}^{-1}$; adults: $0.7 \text{ mg cm}^{-2} \text{ d}^{-1}$); SA represents the exposed skin surface area (children: 2800 cm^2 ; adults: 5700 cm^2); and finally ABS stands for the dermal absorption factor (0.001) [65–67].

For each PTE, the potential non-carcinogenic and carcinogenic risks were calculated according to the following:

$$HI = \sum HQI = \sum \frac{Di}{RfDi} \quad (8)$$

$$TRC = \sum CRi = \sum Di \times SFi \quad (9)$$

The hazard index (HI) is the sum of Hazard Quotients (HQs) and estimates the health risk of different exposure pathways. The reference dose ($RfDi$) ($\text{mg kg}^{-1} \text{ d}^{-1}$) estimates the maximum permissible risk to a human population through daily exposure during a lifetime. The SF and RfD values were obtained from the United States Department of Energy's Risk Assessment Information System RAIS compilation [68] and [12,69] values of HQ and $HI > 1$ indicate a high probability of the occurrence of adverse health effects [63].

For an estimation of the carcinogenic risk, the dose is multiplied by the corresponding slope factor (SF) to produce an estimate of cancer risk. Similarly, the total carcinogenic risk (TCR) was calculated by summing the individual cancer risk across different exposure pathways. The acceptable threshold value of the cancer risk is 1.0×10^{-4} , while the tolerable TCR for regulatory purposes is in the range of 1.0×10^{-6} – 1.0×10^{-4} [64].

3. Results and Discussion

3.1. Soil Geochemical Background Characterization

The geochemical patterns observed in Portuguese soils are generally controlled by lithology, soil type, and mineral occurrences [70].

Considering that the study area locates along the western limb of the Valongo Anticline, an attempt was made to characterize the PTEs concentration in the soils positioned along this limb of the anticline, along the same geological units, for comparison with the concentration values of PTEs in the soils surrounding São Pedro da Cova mine.

Table 1 presents a summary of concentrations in the soils of nine PTEs in this western limb of the regional structure.

The average concentrations of Co, Cr, Cu, Ni, Pb, and Zn are all below the reference values proposed for the Portuguese soils [70], being 19, 43, 35, 43, 34, and 85 mg kg^{-1} , respectively. Despite As being higher than the Portuguese reference value proposed by the National Environmental Agency [49], it presents within the same range of concentrations proposed in the Soil Geochemical Atlas of Portugal [70]. Regarding As, it must be noted that the north of Portugal (where the area of study is located) showed median and average concentrations nearly 20 times higher than in the south or center of the country [70]. In fact, extensive areas present concentrations of As above national [49] and international guidelines [71] in the northern part of the country as a result of the natural geochemical background.

Table 1. Background PTEs concentration in soils from the western limb of the Valongo Anticline, after removing the outliers, in mg kg⁻¹.

	Min. (n = 41)	Max. (n = 41)	Mean (n = 41)	S.D.	Skewness	Kurtosis	1Q	Median	3Q
As	8	88	22	14.38	2.77	12.83	16	18.5	24
Sb	1	18	4.51	3.39	1.96	8.18	2	4	6.75
Co	0.5	9	3.68	2.31	0.44	2.40	2	3	5
Cr	5	36	21.90	21.90	9.10	-0.08	1.79	14	
Cu	4	35	20.37	8.04	-0.15	2.12	1	19.5	28
Mo	0.5	2	0.66	0.31	2.46	10.19	0.5	0.5	1
Ni	0.5	29	12.55	8.38	0.33	1.96	5.75	11	18.5
Pb	13	65	25	9.62	2.13	9.21	19.25	23	28
Zn	5	78	37.13	21.86	0.28	2.00	18.5	35	54

Min—minimum; Max—maximum; S.D.—standard deviation; 1Q—first quartile (25th percentile of data); 3Q—third quartile (75th percentile of the data).

3.2. Environmental Pollution Level Assessment

In order to characterize the environmental pollution of the studied area, the Igeo and C_f indices were calculated for all soil samples and the descriptive statistics for studied PTEs were developed (Table 2).

Table 2. Descriptive statistics for PTE concentrations in the studied soils (in mg kg⁻¹) and determined pollution indices.

	As	Cd	Co	Cr	Cu	Mo	Ni	Pb	Sb	Zn
Minimum (n = 50)	6.30	0.01	0.60	15.00	11.20	0.49	6.60	18.10	1.23	19.10
Maximum (n = 50)	62.80	0.56	32.60	209.00	351.60	6.03	114.60	163.79	46.67	303.10
Mean (n = 50)	22.55	0.11	7.23	74.10	50.18	2.13	24.29	50.22	6.29	96.97
Standard deviation	11.74	0.16	6.32	34.79	51.07	1.39	17.13	30.03	7.94	67.59
Skewness	1.52	1.51	1.75	1.11	4.47	1.04	3.06	1.67	3.33	1.21
Kurtosis	5.82	4.19	6.88	6.44	25.93	3.46	16.50	5.94	15.58	3.73
Crustal abundance [50]	1.5	0.098	10	35	25	1.5	20	20	0.2	71
Regional background	22	<0.50	3.68	21.90	20.37	0.66	12.51	25	4.51	37.13
C_f (with crustal mean as background)	15.03	1.17	0.72	2.12	2.01	1.42	1.21	2.51	31.47	1.37
C_f (with regional background)	1.02	0.46	1.96	3.38	2.46	3.22	1.94	2.01	1.40	2.61
Igeo (with crustal mean as background)	3.16	-1.83	-1.58	0.32	0.09	-0.39	-0.55	0.54	3.79	-0.46
Igeo (with regional background) Igeo	-0.72	-3.19	0.86	0.99	0.39	0.79	0.12	0.22	-0.70	0.48
APA guidelines (agriculture) [49]	11	1	19	67	62	2	37	45	1	290
APA guidelines (urban/industrial) [49]	18	1.2	21	70	95	2	82	120	1.3	290

The studied PTEs present general mean concentrations higher than their respective average earth crustal concentrations, with a special highlight for As that exceeds the crustal average concentrations by 15 times and Sb that exceeds it by 370 times. According to the soil quality standards proposed by the Portuguese Environmental Agency—APA, for agriculture soil in sensitive areas, all soil samples exceeded the reference value for Sb, up to 46.67 mg kg⁻¹ (46 times higher than the reference value), and 94% of the samples showed As concentrations higher than the Portuguese reference, with values that can reach 62.80 mg kg⁻¹ (maximum concentration six times higher than the reference value). Furthermore, 62% of the samples exceed reference limits for Cr and 42% for Mo and Pb. Only 2% of the samples exceeded the Zn limit, 6% in the case of Co, 14% of Ni, and 16% of Cu [44]. There was no record of Cd levels above the Portuguese reference values.

The average C_f and Igeo of the soils based on the average crustal concentrations of the considered PTEs highlights an obvious enrichment in the studied soils. The average values of C_f and Igeo with mean crustal abundance as background occur in the order Sb > As > Pb > Cr > Cu > Mo > Zn > Ni > Cd > Co. The C_f is indicative of low contamination in Co (0.72), moderate contamination in Cd (1.17), Ni (1.21), Mo (1.42), Zn (1.37), Cu (2.01),

Cr (2.12), and Pb (2.51). This parameter classifies the soils as very highly contaminated for As (15.03) and Sb (31.47). Similarly, the Igeo points to unpolluted soils regarding Co (−1.58), Cd (−1.83), Zn (−0.46), Ni (−0.55), and Mo (−0.39), unpolluted to moderately polluted soils in Cu (0.09), Pb (0.54), and Cr (0.32), and is heavily polluted in As (3.16) and Sb (3.79). Figure 3 represents the Igeo determined based on the elemental average crustal concentrations. Both indices determined when using elemental crustal averages point to intense pollution in As and Sb, particularly uphill of the waste pile, in forest areas, without any anthropogenic influence.

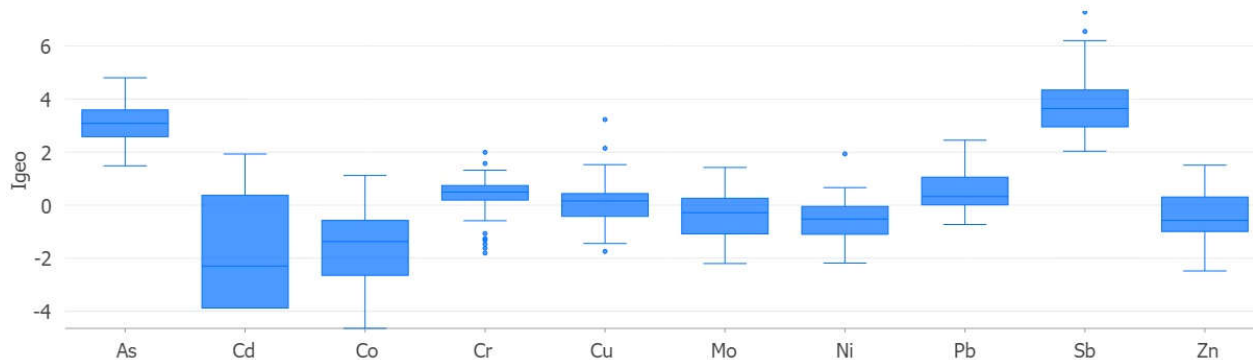


Figure 3. Igeo determined based on average crustal concentrations of metals and metalloids.

The average C_f and Igeo of the soils surrounding the mine were also determined considering the estimated regional background for the western limb of the Valongo Belt. Figure 4 represents the Igeo calculated for the studied samples based on the determined regional background. The results presented a substantial reduction in the intensity of the pollution indices applied to the studied soils as, for most PTEs, the Igeo regarding regional background ranges between unpolluted to moderately polluted (Figure 4).

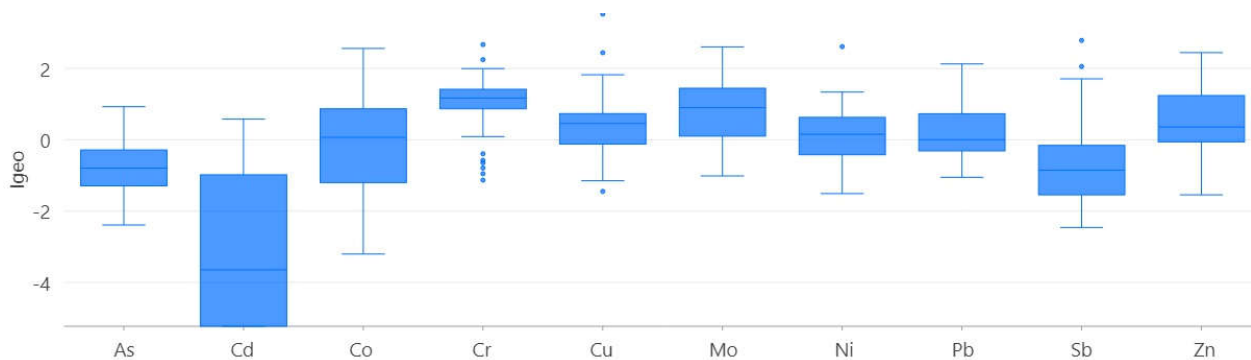


Figure 4. Igeo of metals and metalloids defined based on the determined regional geochemical background.

Therefore, it is considered that the most appropriate geochemical baseline to be used for the environmental indices in this study is the regional geochemical background, as concentrations of As and Sb in northern Portugal are significantly higher than crustal averages [70], and are possibly enhanced by the mineralization events that occurred in the area. The Valongo Anticline is known by multiple mineral occurrences, including Au and Sb [72–74].

According to the regional background, the average values of C_f consider an enrichment according to the following order: Cr > Mo > Zn > Cu > Pb > Co > Ni > Sb > As > Cd.

They present low contamination in Cd (0.46), are moderately contaminated in As (1.02), Sb (1.40), Ni (1.94), Co (1.96), Pb (2.01), Cu (2.46), and Zn (2.61). The soils present high contamination in Mo (3.22) and Cr (3.38). The Igeo follows a similar trend, with soils

unpolluted in Cd (−3.19), As (−0.72) and unpolluted to moderately polluted in Sb (−0.70), Ni (0.12), Pb (0.22), Cu (0.39), Zn (0.48), Mo (0.79), Co (0.86), and Cr (0.99).

Table 3 presents the summary of the PTE concentrations in different areas surrounding the waste pile, and the respective calculated Igeo values according to the land use. The soils located along the waste pile runoff areas and drainage basin, are considered unpolluted in Co (−0.02), Cd (−2.34), Ni (−0.11), As (−0.59), and Sb (−0.64), and unpolluted to moderately polluted in Cu (0.11), Zn (0.68), Pb (0.33), Cr (0.41), and Mo (0.27), according to the Igeo. The highest Igeo value obtained for Zn along the runoff area is compatible with observations from previous studies, as leaching tests conducted previously in waste pile materials, included Zn as one of the elements with highest concentrations in leachates [39], therefore with great mobility potential. A comparison between horizons affected and unaffected by combustion in these waste piles showed that leaching of some elements seemed to be temperature dependent, with higher concentrations in leachable elements found in self-burning coal waste samples, when compared with the unburned material. Zinc was highlighted as increasing in leachates of the horizons most intensely affected by combustion, as well Mn and Al [42].

Table 3. Descriptive statistics for PTEs concentrations in the subsets of the studied soils (in mg kg^{−1}), according to the land use and the corresponding Igeo calculated considering the determined regional geochemical background.

Soil Affected by Waste Pile Drainage										
	As	Cd	Co	Cr	Cu	Mo	Ni	Pb	Sb	Zn
Minimum (n = 8)	12.9	0.01	1.6	15	13.8	0.52	9.7	27.5	1.35	47.8
Maximum (n = 8)	36.1	0.56	11.5	111	100.4	3.51	32.2	84.8	46.67	303.1
Mean (n = 8)	23.46	0.15	6.74	56.5	41.91	1.62	19.85	53.99	9.42	115.65
Standard deviation	8.96	0.2	3.58	31.32	28.5	1.17	8.63	19.04	15.46	80.63
Skewness	0.24	1.27	−0.05	0.26	1.14	0.7	0.22	0.23	2.05	1.78
Kurtosis	1.75	3.08	1.51	2.3	3.17	1.94	1.45	1.99	5.54	4.88
Igeo	−0.59	−2.34	−0.02	0.41	0.11	0.27	−0.11	0.33	−0.64	0.68
Forestry Soil Uphill from the Waste Pile										
	As	Cd	Co	Cr	Cu	Mo	Ni	Pb	Sb	Zn
Minimum (n = 24)	11.3	0.01	0.6	22	11.2	0.52	8.1	18.1	1.54	19.1
Maximum (n = 24)	62.8	0.46	15.6	209	108.2	6.03	114.6	105.53	16.26	243.7
Mean (n = 24)	25.73	0.06	5.61	85.44	39.15	2.76	25.24	39.5	5.45	68.82
Standard deviation	13.54	0.12	4.72	33.68	19.48	1.55	2.24	22.14	4.26	52.48
Skewness	1.43	2.45	0.86	1.88	1.79	0.52	3.14	1.97	1.43	1.98
Kurtosis	4.68	7.71	2.39	8.66	7.42	2.39	13.75	6.13	4	6.77
Igeo	−0.48	−4.04	−0.56	1.27	0.2	1.29	0.14	−0.09	−0.63	−0.04
Urban Soil Uphill from the Waste Pile										
	As	Cd	Co	Cr	Cu	Mo	Ni	Pb	Sb	Zn
Minimum (n = 15)	6.3	0.01	2.4	15	22.2	0.53	8.2	29.47	1.35	56.3
Maximum (n = 15)	36.1	0.42	32.6	111	351.6	3.51	44.9	163.79	12.15	252.8
Mean (n = 15)	18.35	0.17	8.85	66.2	82.81	1.48	23.77	74.19	4.35	141.42
Standard deviation	7.45	0.12	7.46	31.08	82.14	0.81	11.38	36.85	2.62	64.19
Skewness	0.62	0.39	2.26	−0.37	2.58	1.12	0.44	0.99	1.79	0.3
Kurtosis	3.28	2.42	8.04	1.86	8.91	3.7	2.36	3.37	6.32	1.94
Igeo	−0.96	−1.76	0.33	0.79	1.05	0.39	0.17	0.82	−0.83	1.19

Previous studies have not indicated a significant soils acidification in these soils [44]; in fact, the acid generation potential of this waste pile indicates it is moderately prone to form acid mine drainage [40].

The forest soil, located predominantly upstream from the drainage basin and higher than the waste pile, has demonstrated Igeo values that classify these soils as unpolluted to moderately polluted in Cu (0.2), Ni (0.14), Cr (1.27), and Mo (1.29), and unpolluted in Cd (−4.04), Sb (−0.63), Co (−0.56), As (−0.48), Pb (−0.09), and Zn (−0.04).

The urban areas, located outside the mine drainage basin, present soils classified in terms of Igeo as unpolluted in As (−0.96), Sb (−0.83), and Cd (−1.76), and unpolluted to moderately polluted in Ni (0.17), Co (0.33), Mo (0.39), Cr (0.79), Pb (0.82), and Zn (1.19).

The RI was calculated for the PTEs, assessing the potential ecological risks for the various soil samples surrounding the mine, again following two approaches, the first using the elemental crustal abundance [50], and the second based on the determined regional background. Table 4 presents the averages for the individual ecologic risk index E_r^i as well as the cumulative risk index RI.

Table 4. General E_r^i values determined for the PTEs in the studied samples and the correspondent RI values determined based on elemental crustal averages and the determined regional background.

Potential Ecological Risk of Individual Metals and Metalloids (E_r^i)								Ecological Risk (RI)
Using regional background to determine C_f								
As	Cd	Cr	Cu	Ni	Pb	Sb	Zn	78.6
10.3	13.7	10.2	12.3	9.70	10.0	9.77	2.61	
13	17	13	16	12	13	12	3	Contribution (%)
Using crustal average to determine C_f								
150	35.0	6.35	10.0	6.07	12.6	220	1.37	442
34	8	1	2	1	3	50	0	Contribution (%)

Considering the crustal abundance as the geochemical baseline in the C_f determination, the E_r^i values of each individual decrease in the following order Sb > As > Cd > Cu > Pb > Cr > Ni > Zn. From the studied toxic elements, most E_r^i values were below 40, therefore considered low risk. However, As presents E_r^i of 150, consistent with considerable risk, and Sb registers an E_r^i of 220, which could be considered as a high ecological risk. Regarding the RI, the soils that surround the mine can be considered a considerable ecological risk (RI = 442).

However, taking into consideration the determined regional background for the C_f definition, the E_r^i values decrease in the following order Cd > Cu > As > Cr > Pb > Sb > Ni > Zn, and all the studied toxic elements are lower than 40; therefore, these elements could be considered as low risk. For this case, the assessed RI is below the minimum threshold of 150 and is considered low risk (RI = 79).

The individual RI calculated from the geochemical results of each soil sample allowed its spatial distribution modelling using geostatistical algorithms, namely ordinary kriging. The results for the RI spatial distribution determined based on elemental crustal averages are presented in Figure 5, and the RI spatial distribution determined based on the regional geochemical background is represented in Figure 6.

In Figure 5, from the soils collected around the waste pile, only 2% were considered low risk, 40% of the samples ranked as moderate risk, 36% of the samples presented a considerable risk, and 22% as high risk (with RI up to 1962).

Comparing the RI determined using the crustal average (Figure 5) and the regional geochemical background (Figure 6), a very distinct pattern can be observed. The highest RI values in Figure 5 are located east of the mine waste pile and uphill, which could not suggest any influence of the waste pile runoff. The elements that mostly contribute to

the determined RI are Sb (50%) and As (34%). Previous research [44] pointed out that the highest concentrations of As and Sb were coincident with this zone of increased RI, and in this area, As and Sb were pointed to having pedological sources, related to a natural enhancement on the regional background of these elements, as the underlying bedrock are geological units that belong to the Valongo Anticline, which is well-known for the existence of for dozens of mineral Au and Au-Sb occurrences [72–74].

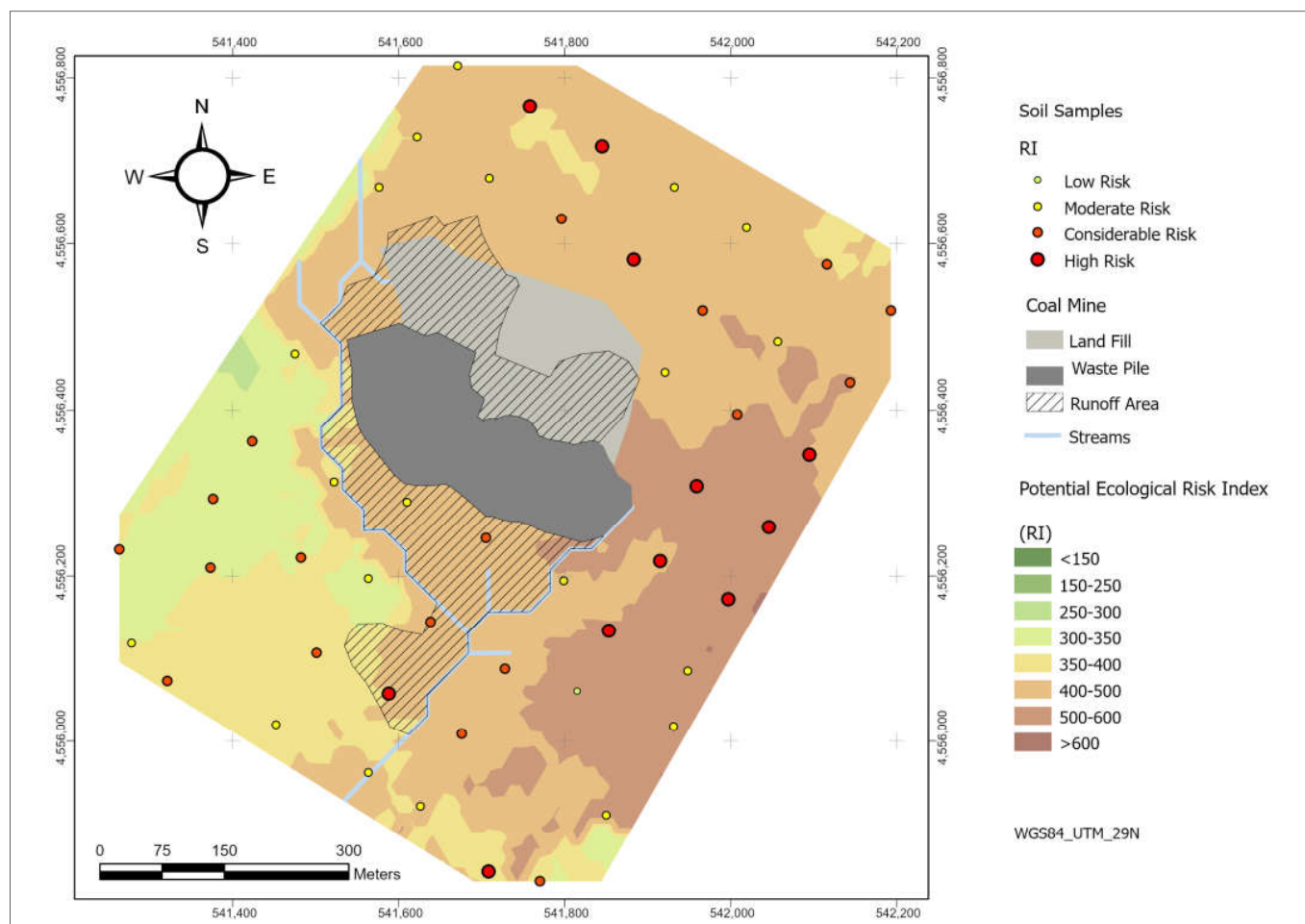


Figure 5. Potential ecological risk index determined using crustal average as the geochemical baseline.

When the same methodologies are applied in RI calculation using the determined regional background, the geochemical signatures of the soils are closer, and it is no longer possible to verify a large asymmetry in the contributions of each metal and metalloid to the total RI. Table 4 highlights the individual PTEs contributions to combined RI, Cd and Cu have the highest contributions with 17% and 18%, respectively, followed by As, Cr and Pb, with contributions of 13%, and Ni and Sb with contributions of 12%. The lowest contributor for RI is Zn, with a 3% contribution.

From the soil samples in the vicinity of the mine, 90% of them presented low risk (RI < 150), only five samples presented a moderate ecological risk, with RI values ranging from 151 to 197, and none of these samples was located near the waste pile runoff areas or drainage, suggesting that the mine does not promote significant ecological risk to the surrounding soils.

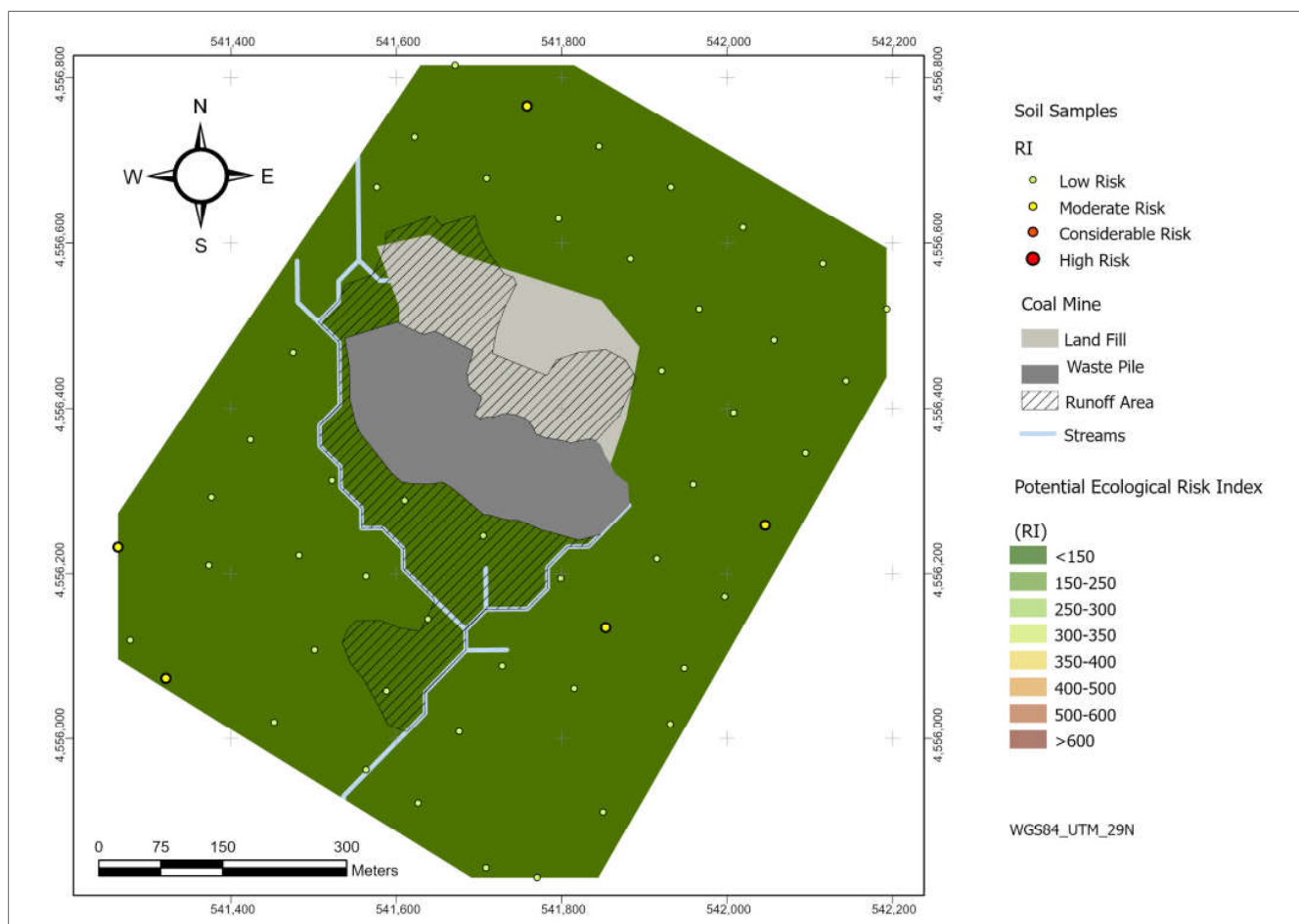


Figure 6. Potential ecological risk index determined using regional background as the geochemical baseline.

3.3. Human Health Risk Assessment Index

Table 5 compiles the data about the non-carcinogenic and carcinogenic risk via ingestion, inhalation, and dermal contact of As, Cd, Cr, Cu, Ni, Pb, and Zn, in children and adults. Total elemental concentrations were used for health risk assessment in this study; despite not being as close to the actual hazard they pose, it was a more conservative approach.

Regarding the non-carcinogenic risk, the total exposure HI resulting from ingestion, inhalation, and dermal contact, for the considered PTEs, is significantly lower than 1, which suggests that there is no potential human health risk for children or adults. Nevertheless, HI values are higher in children than adults, suggesting these are the most vulnerable to exposure. The total HI values for children is 7.99×10^{-1} and for adults is 1.26×10^{-1} .

The highest contribution to HI values is mostly attributed to As, followed by Cr and Pb, considering children the respective contributions were 62% As followed by 23% Cr and 12% Pb. Regarding adults, the respective percentages were 46% As, 42% Cr, and 10% Pb. The non-carcinogenic risk for children increases as follows, Cd < Zn < Ni < Cu < Pb < Cr < As. Risk regarding adult exposure follows the same trend; however, Zn constitutes the lower risk. The main hazard exposure pathways for both children and adults are ingestion, followed by dermal contact, and finally inhalation. The only exception is regarding Cr, as the main exposure pathway for adults is dermal ($HQ = 3.47 \times 10^{-2}$), followed by ingestion ($HQ = 1.74 \times 10^{-2}$). The results indicate that ingestion is a significant exposure pathway posing a higher risk for direct ingestion of soil and dust than adults, as reported in identical studies [12,75,76]. This is because children are exposed by playing outdoors on the ground with toys and hand-to-mouth behaviors [14,18].

Table 5. Non-carcinogenic and carcinogenic risks via ingestion, inhalation, and dermal contact of As, Cd, Cr, Cu, Ni, Pb, and Zn, in children and adults in the soils that surround São Pedro da Cova mine waste pile.

Element	As non	As carc	Cd non	Cd carc	Cr non	Cr carc	Cu	Ni non	Ni carc	Pb	Zn	Total
C (mg kg ⁻¹)	22.55	22.55	0.11	0.11	74.1	74.1	50.18	24.29	24.29	50.22	96.97	
Ing RfD	3.00×10^{-4}		1.00×10^{-3}		3.00×10^{-3}		4.00×10^{-2}	2.00×10^{-2}		3.50×10^{-3}	3.00×10^{-1}	
Inhal RfD	3.00×10^{-4}		1.00×10^{-3}		2.86×10^{-5}		4.20×10^{-2}	2.06×10^{-2}		3.52×10^{-3}	3.00×10^{-1}	
Dermal RfD	1.23×10^{-4}		1.00×10^{-5}		6.00×10^{-5}		1.20×10^{-2}	5.40×10^{-3}		5.25×10^{-4}	6.00×10^{-2}	
Oral SF		$1.50 \times 10^{+0}$		3.80×10^{-1}		5.01×10^{-1}			$1.70 \times 10^{+0}$			
Inhal SF		$1.51 \times 10^{+1}$		$6.30 \times 10^{+0}$		$4.20 \times 10^{+1}$			8.40×10^{-1}			
Dermal SF		$1.50 \times 10^{+0}$		3.80×10^{-1}		$2.00 \times 10^{+1}$			$4.25 \times 10^{+1}$			
Children												
HQing	4.94×10^{-1}		7.23×10^{-4}		1.62×10^{-1}		8.25×10^{-3}	7.99×10^{-3}		9.43×10^{-2}	2.13×10^{-3}	7.70×10^{-1}
HQInh	1.39×10^{-5}		2.03×10^{-8}		4.78×10^{-4}		2.20×10^{-7}	2.17×10^{-7}		2.63×10^{-6}	5.96×10^{-8}	4.95×10^{-4}
HQdermal	3.38×10^{-3}		2.03×10^{-4}		2.27×10^{-2}		7.70×10^{-5}	8.28×10^{-5}		1.76×10^{-3}	2.98×10^{-5}	2.83×10^{-2}
HI	4.98×10^{-1}		9.26×10^{-4}		1.86×10^{-1}		8.33×10^{-3}	8.07×10^{-3}		9.61×10^{-2}	2.16×10^{-3}	7.99×10^{-1}
Contribution (%)	62.3		0.12		23.24		1.04	1.01		12.03	0.27	
CRing		1.91×10^{-5}		2.36×10^{-8}		2.09×10^{-5}			2.33×10^{-5}			6.33×10^{-5}
CRinh		5.38×10^{-9}		1.10×10^{-11}		4.92×10^{-8}			3.23×10^{-10}			5.49×10^{-8}
CRdermal		5.34×10^{-8}		6.60×10^{-11}		2.34×10^{-6}			1.63×10^{-6}			4.02×10^{-6}
TCR		1.91×10^{-5}		2.36×10^{-8}		2.33×10^{-5}			2.49×10^{-5}			6.74×10^{-5}
Contribution (%)		28.4		0.04		34.6			37.0			
Adults												
HQing	5.30×10^{-2}		7.75×10^{-5}		1.74×10^{-2}		8.84×10^{-4}	8.56×10^{-4}		1.01×10^{-2}	2.28×10^{-4}	8.25×10^{-2}
HQInh	7.79×10^{-6}		1.14×10^{-8}		2.68×10^{-4}		1.24×10^{-7}	1.22×10^{-7}		1.48×10^{-6}	3.35×10^{-8}	2.78×10^{-4}
HQdermal	5.15×10^{-3}		3.09×10^{-4}		3.47×10^{-2}		1.18×10^{-4}	1.26×10^{-4}		2.69×10^{-3}	4.54×10^{-5}	4.32×10^{-2}
HI	5.81×10^{-2}		3.87×10^{-4}		5.24×10^{-2}		1.00×10^{-3}	9.82×10^{-4}		1.28×10^{-2}	2.73×10^{-4}	1.26×10^{-1}
Contribution (%)	46.14		0.31		41.6		0.80	0.78		10.16	0.22	
CRing		8.17×10^{-6}		1.01×10^{-8}		8.97×10^{-6}			9.97×10^{-6}			2.71×10^{-5}
CRinh		1.21×10^{-8}		2.46×10^{-11}		1.11×10^{-7}			7.25×10^{-10}			1.23×10^{-7}
CRdermal		3.26×10^{-7}		4.03×10^{-10}		1.43×10^{-5}			9.95×10^{-6}			2.46×10^{-5}
TCR		8.51×10^{-6}		1.05×10^{-8}		2.34×10^{-5}			1.99×10^{-5}			5.18×10^{-5}
Contribution (%)		16.4		0.02		45.1			38.5			

non—noncarcinogens; car—carcinogens; C—concentration average; Ing RfD—ingestion reference dose; Inhal RfD—inhalation reference dose; Dermal RfD—dermal reference dose; Oral SF—oral slope factor; Inhal SF—inhalation slope factor; Dermal SF—dermal slope factor; HQing—ingestion hazard quotient; HQInh—inhalation hazard quotient; HQdermal—dermal hazard quotient; HI—hazard index; CRing—ingestion carcinogenic risk; CRinh—inhalation carcinogenic risk; CRdermal—dermal carcinogenic risk; TCR—total carcinogenic risk.

The carcinogenic risk was also inferred according to the three preferential exposure pathways. The determined carcinogenic risk for the studied elements is lower than the maximum USEPA acceptance risk threshold of 1.0×10^{-4} [64]. The TRC for children was 6.74×10^{-5} , with main contributions of 37% Ni, 35% Cr, and 28% As. Arsenic for the adults the determined TRC was 5.18×10^{-5} , with the highest contributions of Cr (45%), Ni (39%), and As (16.4%). The TRCs calculated for both children and adults are within the tolerable range for regulatory purposes (1.0×10^{-6} – 1.0×10^{-4}) [64].

Regarding carcinogenic risk, similar to what occurred with HI, ingestion seems to constitute the main exposure, except for Cr in adults, which registers a higher RC for dermal contact.

4. Conclusions

The results obtained in this study provided useful knowledge about the ecological and human health risks associated with contaminant exposure in the soil surrounding an abandoned coal mine and a waste pile that has been self-burning for over 17 years. Furthermore, this model can provide references for the population and regional government for scientific-based decision-making.

In Portugal, many studies were devoted to the study of the mineralogical and geochemical transformations of the residues deposited in different coal waste piles affected by combustion; however, this is a pioneer study regarding the contamination of the soils surrounding these waste piles.

The methodology applied, comparing two approaches as a geochemical baseline, highlighted the absolute necessity of an adequate regional geochemical characterization, particularly in the case of studies surrounding mining areas, since these present natural enhancement of different elements as a result of the regional mineralizing events. Effort must be made to calculate the pollution indexes by comparing them with the regional geochemical background, otherwise, local geochemical anomalies, easily explained by mineralization, shall be highlighted as polluted areas. Elemental crustal abundance or concentration in soil averages in the world or Europe is inappropriate for the soil environmental characterization in mining areas. The pollution indices applied in this study presented a substantial reduction when determined by taking into account the regional geochemical background.

In the studied soils, the Igeo determined considering regional background ranges between unpolluted to moderately polluted. Regarding the ecological risk, 90% of the samples presented a low risk, and only five samples presented moderate ecological risk, samples 2, 28, 37, 46 and 54, with low values on the rank (RI ranging between 151 and 197). Nevertheless, these samples are not located near the waste pile runoff areas or drainage, suggesting that the mine waste pile does not promote a significant ecological risk.

Regarding the non-carcinogenic risk, the total exposure HI resultant from ingestion, inhalation, and dermal contact for the considered PTEs, suggests that there is no potential human health risk for children or adults in the studied soils. The determined carcinogenic risk for the studied elements was also low, since TRC calculated for both children and adults was within the tolerable range for regulatory purposes.

Considering that this study is the reflex of a local study, with some particularities as being integrated in a larger mining district, where not only coal was exploited but also gold and antimony, and given the fact that combustion is still undergoing, reservations must be made concerning the universal application of these conclusions to other prospects. In the future, the study area would benefit from the continuity of the environmental monitoring, including soils and waters geochemical surveys, thermal infrared scanning to determine the evolution of combustion areas as well as altimetric monitoring to control general subsidence of the region.

Author Contributions: Conceptualization, P.S. and D.F.; methodology, P.S., J.R., J.E.M. and D.F.; software, P.S.; validation, P.S., J.R., J.E.M. and D.F.; formal analysis, P.S.; investigation, P.S.; resources, P.S. and D.F.; data curation, P.S.; writing—original draft preparation, P.S.; writing—review and editing, P.S., J.R., J.E.M. and D.F.; visualization, P.S.; supervision, D.F.; project administration, D.F.; funding acquisition, D.F. All authors have read and agreed to the published version of the manuscript.

Funding: This work was funded through the Foundation for Science and Technology, through the CoalMine project with the ref. POCI-01-0145-FEDER-030138, 02-SAICT-2017, by FEDER funding through the COMPETE 2020 programme and framed within the ICT activities (projects UIDB/04683/2020 and UIDP/04683/2020).

Data Availability Statement: Not applicable.

Acknowledgments: The authors want to acknowledge João Rocha for the support given in several steps of the CoalMine project.

Conflicts of Interest: The authors declare no conflict of interest.

References

1. Marove, C.A.; Sotozono, R.; Tangviroon, P.; Tabelin, C.B.; Igarashi, T. Assessment of Soil, Sediment and Water Contaminations around Open-Pit Coal Mines in Moatize, Tete Province, Mozambique. *Environ. Adv.* **2022**, *8*, 100215. [[CrossRef](#)]
2. Liu, X.; Shi, H.; Bai, Z.; Zhou, W.; Liu, K.; Wang, M.; He, Y. Heavy Metal Concentrations of Soils near the Large Opencast Coal Mine Pits in China. *Chemosphere* **2020**, *244*, 125360. [[CrossRef](#)]
3. Fdez-Ortiz de Vallejuelo, S.; Gredilla, A.; da Boit, K.; Teixeira, E.C.; Sampaio, C.H.; Madariaga, J.M.; Silva, L.F.O. Nanominerals and Potentially Hazardous Elements from Coal Cleaning Rejects of Abandoned Mines: Environmental Impact and Risk Assessment. *Chemosphere* **2017**, *169*, 725–733. [[CrossRef](#)] [[PubMed](#)]
4. Li, Y.; Zhou, S.; Zhu, Q.; Li, B.; Wang, J.; Wang, C.; Chen, L.; Wu, S. One-Century Sedimentary Record of Heavy Metal Pollution in Western Taihu Lake, China. *Environ. Pollut.* **2018**, *240*, 709–716. [[CrossRef](#)]
5. Chen, L.; Zhou, S.; Shi, Y.; Wang, C.; Li, B.; Li, Y.; Wu, S. Heavy Metals in Food Crops, Soil, and Water in the Lihe River Watershed of the Taihu Region and Their Potential Health Risks When Ingested. *Sci. Total Environ.* **2018**, *615*, 141–149. [[CrossRef](#)] [[PubMed](#)]
6. Sadiku, M.; Kadriu, S.; Kelmendi, M.; Latifi, L. Impact of Artana Mine on Heavy Metal Pollution of the Marec River in Kosovo. *Min. Miner. Depos.* **2021**, *15*, 18–24. [[CrossRef](#)]
7. Kadriu, S.; Sadiku, M.; Kelmend, M.; Sadriu, E. Studying the Heavy Metals Concentration in Discharged Water from the Trepça Mine and Flotation, Kosovo. *Min. Miner. Depos.* **2020**, *14*, 47–52. [[CrossRef](#)]
8. Skrobala, V.; Popovych, V.; Tyndyk, O.; Voloshchysyn, A. Chemical Pollution Peculiarities of the Nadiya Mine Rock Dumps in the Chervonohrad Mining District, Ukraine. *Min. Miner. Depos.* **2022**, *16*, 71–79. [[CrossRef](#)]
9. Pavlychenko, A.; Kovalenko, A. The Investigation of Rock Dumps Influence to the Levels of Heavy Metals Contamination of Soil. In *Mining of Mineral Deposits*; CRC Press: Boca Raton, FL, USA, 2013; pp. 237–238.
10. Finkelman, R.B.; Palmer, C.A.; Wang, P. Quantification of the Modes of Occurrence of 42 Elements in Coal. *Int. J. Coal Geol.* **2018**, *185*, 138–160. [[CrossRef](#)]
11. Finkelman, R.B. Potential Health Impacts of Burning Coal Beds and Waste Banks. *Int. J. Coal Geol.* **2004**, *59*, 19–24. [[CrossRef](#)]
12. Li, H.; Ji, H. Chemical Speciation, Vertical Profile and Human Health Risk Assessment of Heavy Metals in Soils from Coal-Mine Brownfield, Beijing, China. *J. Geochem. Explor.* **2017**, *183*, 22–32. [[CrossRef](#)]
13. Querol, X.; Zhuang, X.; Font, O.; Izquierdo, M.; Alastuey, A.; Castro, I.; van Drooge, B.L.; Moreno, T.; Grimalt, J.O.; Elvira, J.; et al. Influence of Soil Cover on Reducing the Environmental Impact of Spontaneous Coal Combustion in Coal Waste Gobs: A Review and New Experimental Data. *Int. J. Coal Geol.* **2011**, *85*, 2–22. [[CrossRef](#)]
14. Shahab, A.; Zhang, H.; Ullah, H.; Rashid, A.; Rad, S.; Li, J.; Xiao, H. Pollution Characteristics and Toxicity of Potentially Toxic Elements in Road Dust of a Tourist City, Guilin, China: Ecological and Health Risk Assessment. *Environ. Pollut.* **2020**, *266*, 115419. [[CrossRef](#)]
15. Kumar, V.; Sharma, A.; Kaur, P.; Singh Sidhu, G.P.; Bali, A.S.; Bhardwaj, R.; Thukral, A.K.; Cerda, A. Pollution Assessment of Heavy Metals in Soils of India and Ecological Risk Assessment: A State-of-the-Art. *Chemosphere* **2019**, *216*, 449–462. [[CrossRef](#)] [[PubMed](#)]
16. Kusin, F.M.; Awang, N.H.C.; Hasan, S.N.M.S.; Rahim, H.A.A.; Azmin, N.; Jusop, S.; Kim, K.W. Geo-Ecological Evaluation of Mineral, Major and Trace Elemental Composition in Waste Rocks, Soils and Sediments of a Gold Mining Area and Potential Associated Risks. *Catena* **2019**, *183*, 104229. [[CrossRef](#)]
17. Bhuiyan, M.A.H.; Parvez, L.; Islam, M.A.; Dampare, S.B.; Suzuki, S. Heavy Metal Pollution of Coal Mine-Affected Agricultural Soils in the Northern Part of Bangladesh. *J. Hazard. Mater.* **2010**, *173*, 384–392. [[CrossRef](#)]
18. Ma, L.; Xiao, T.; Ning, Z.; Liu, Y.; Chen, H.; Peng, J. Pollution and Health Risk Assessment of Toxic Metal(Loid)s in Soils under Different Land Use in Sulphide Mineralized Areas. *Sci. Total Environ.* **2020**, *724*, 138176. [[CrossRef](#)]

19. Candeias, C.; Ferreira da Silva, E.; Salgueiro, A.R.; Pereira, H.G.; Reis, A.P.; Patinha, C.; Matos, J.X.; Ávila, P.H. The Use of Multivariate Statistical Analysis of Geochemical Data for Assessing the Spatial Distribution of Soil Contamination by Potentially Toxic Elements in the Aljustrel Mining Area (Iberian Pyrite Belt, Portugal). *Environ. Earth Sci.* **2011**, *62*, 1461–1479. [[CrossRef](#)]
20. Durães, N.; Portela, L.; Sousa, S.; Patinha, C.; Ferreira da Silva, E. Environmental Impact Assessment in the Former Mining Area of Regoufe (Arouca, Portugal): Contributions to Future Remediation Measures. *Int. J. Environ. Res. Public Health* **2021**, *18*, 1180. [[CrossRef](#)]
21. Candeias, C.; Ferreira da Silva, E.; Ávila, P.; Teixeira, J. Identifying Sources and Assessing Potential Risk of Exposure to Heavy Metals and Hazardous Materials in Mining Areas: The Case Study of Panasqueira Mine (Central Portugal) as an Example. *Geosciences* **2014**, *4*, 240–268. [[CrossRef](#)]
22. Ferreira da Silva, E.F.; Freire Ávila, P.; Salgueiro, A.R.; Candeias, C.; Garcia Pereira, H. Quantitative–Spatial Assessment of Soil Contamination in S. Francisco de Assis Due to Mining Activity of the Panasqueira Mine (Portugal). *Environ. Sci. Pollut. Res.* **2013**, *20*, 7534–7549. [[CrossRef](#)]
23. Antunes, M.; Teixeira, R.; Valente, T.; Santos, A. Geo-Accumulation Indexes of Trace Elements in Sediments from Uranium Environments (Central Portugal). In *New Prospects in Environmental Geosciences and Hydrogeosciences*; Springer: Cham, Switzerland, 2022; pp. 215–217.
24. Kowalska, J.B.; Mazurek, R.; Gašiorek, M.; Zaleski, T. Pollution Indices as Useful Tools for the Comprehensive Evaluation of the Degree of Soil Contamination—A Review. *Environ. Geochem. Health* **2018**, *40*, 2395–2420. [[CrossRef](#)]
25. Muller, G. Index of Geoaccumulation in Sediments of the Rhine River. *Geo J.* **1969**, *2*, 108–118.
26. Abraham, G.M.S.; Parker, R.J. Assessment of Heavy Metal Enrichment Factors and the Degree of Contamination in Marine Sediments from Tamaki Estuary, Auckland, New Zealand. *Environ. Monit. Assess.* **2007**, *136*, 227–238. [[CrossRef](#)] [[PubMed](#)]
27. Hakanson, L. An Ecological Risk Index for Aquatic Pollution Control: a Sedimentological Approach. *Water Res.* **1980**, *14*, 975–1001. [[CrossRef](#)]
28. Pejman, A.; Nabi Bidhendi, G.; Ardestani, M.; Saeedi, M.; Baghvand, A. A New Index for Assessing Heavy Metals Contamination in Sediments: A Case Study. *Ecol. Indic.* **2015**, *58*, 365–373. [[CrossRef](#)]
29. Duodu, G.O.; Goonetilleke, A.; Ayoko, G.A. Comparison of Pollution Indices for the Assessment of Heavy Metal in Brisbane River Sediment. *Environ. Pollut.* **2016**, *219*, 1077–1091. [[CrossRef](#)] [[PubMed](#)]
30. Connor, J.J.; Shacklette, H.T. *Background Geochemistry of Some Soils, Plants and Vegetables in Conterminous United States*; United States Government Printing Office: Washington, DC, USA, 1975.
31. Kabata-Pendias, A. *Trace Elements in Soils and Plants*, 4th ed.; Taylor & Francis Group: Boca Raton, FL, USA; London, UK; New York, NY, USA, 2011.
32. Gazley, M.F.; Martin, A.P.; Turnbull, R.E.; Frontin-Rollet, G.; Strong, D.T. Regional Patterns in Standardised and Transformed Pathfinder Elements in Soil Related to Orogenic-Style Mineralisation in Southern New Zealand. *J. Geochem. Explor.* **2020**, *217*, 106593. [[CrossRef](#)]
33. Hawkes, H.E.; Webb, J.S. *Geochemistry in Mineral Exploration*; Harper: New York, NY, USA; Evanston: New York, NY, USA, 1963.
34. *ISO 11760*; Classification of Coals, 1st ed. International Organization for Standardization: Geneva, Switzerland, 2005; p. 9.
35. Ribeiro, J.; Da Silva, E.F.; Flores, D. Burning of Coal Waste Piles from Douro Coalfield (Portugal): Petrological, Geochemical and Mineralogical Characterization. *Int. J. Coal Geol.* **2010**, *81*, 359–372. [[CrossRef](#)]
36. Ribeiro, J.; Da Silva, E.F.; De Jesus, A.P.; Flores, D. Petrographic and Geochemical Characterization of Coal Waste Piles from Douro Coalfield (NW Portugal). *Int. J. Coal Geol.* **2011**, *87*, 226–236. [[CrossRef](#)]
37. Ribeiro, J.; Silva, T.; Mendonça Filho, J.G.; Flores, D. Polycyclic Aromatic Hydrocarbons (PAHs) in Burning and Non-Burning Coal Waste Piles. *J. Hazard. Mater.* **2012**, *199–200*, 105–110. [[CrossRef](#)] [[PubMed](#)]
38. Ribeiro, J.; Sant’Ovaia, H.; Gomes, C.; Ward, C.; Flores, D. Mineralogy and Magnetic Parameters of Materials Resulting from the Mining and Consumption of Coal from the Douro Coalfield, Northwest Portugal. In *Coal and Peat Fires: A Global Perspective*; Elsevier Inc.: Amsterdam, The Netherlands, 2014; Volume 3, pp. 494–508, ISBN 9780444595119.
39. Ribeiro, J.; Flores, D. Occurrence, Leaching, and Mobility of Major and Trace Elements in a Coal Mining Waste Dump: The Case of Douro Coalfield, Portugal. *Energy Geosci.* **2021**, *2*, 121–128. [[CrossRef](#)]
40. Çelebi, E.E.; Ribeiro, J. Prediction of Acid Production Potential of Self-Combusted Coal Mining Wastes from Douro Coalfield (Portugal) with Integration of Mineralogical and Chemical Data. *Int. J. Coal Geol.* **2023**, *265*, 104152. [[CrossRef](#)]
41. Teodoro, A.; Santos, P.; Espinha Marques, J.; Ribeiro, J.; Mansilha, C.; Melo, A.; Duarte, L.; Rodrigues De Almeida, C.; Flores, D. An Integrated Multi-Approach to Environmental Monitoring of a Self-Burning Coal Waste Pile: The São Pedro Da Cova Mine (Porto, Portugal) Study Case. *Environments* **2021**, *8*, 48. [[CrossRef](#)]
42. Espinha Marques, J.E.; Martins, V.; Santos, P.; Ribeiro, J.; Mansilha, C.; Melo, A.; Rocha, F.; Flores, D. Changes Induced by Self-Burning in Technosols from a Coal Mine Waste Pile: A Hydrogeological Approach. *Geosciences* **2021**, *11*, 195. [[CrossRef](#)]
43. Mansilha, C.; Melo, A.; Flores, D.; Ribeiro, J.; Ramalheira Rocha, J.; Martins, V.; Santos, P.; Marques, J.E.; Ritter, F. Irrigation with Coal Mining Effluents: Sustainability and Water Quality Considerations (São Pedro Da Cova, North Portugal). *Water* **2021**, *13*, 2157. [[CrossRef](#)]
44. Santos, P.; Espinha Marques, J.; Ribeiro, J.; Mansilha, C.; Melo, A.; Fonseca, R.; Sant’Ovaia, H.; Flores, D. Geochemistry of Soils from the Surrounding Area of a Coal Mine Waste Pile Affected by Self-Burning (Northern Portugal). *Minerals* **2023**, *13*, 28. [[CrossRef](#)]

45. de Sousa, M.J.L.; Wagner, R.H. General Description of the Terrestrial Carboniferous Basins in Portugal and History of Investigations. In *The Carboniferous of Portugal: Memórias dos Serviços Geológicos de Portugal*; Lemos de Sousa, M.J., Oliveira, J.T., Eds.; Direcção-Geral de Geologia e Minas: Lisboa, Portugal, 1983; pp. 117–126.
46. Correia, P.; Šimůnek, Z.; Sá, A.A.; Flores, D. A New Late Pennsylvanian Floral Assemblage from the Douro Basin, Portugal. *Geol. J.* **2018**, *53*, 2507–2531. [[CrossRef](#)]
47. De Jesus, A.P. Carboniferous Intermontane Basins of Portugal. In *The Geology of Iberia: A Geodynamic Approach*; Oliveira, J., Quesada, C., Eds.; Springer Nature Switzerland AG: Cham, Switzerland, 2019; Volume 2, pp. 402–408.
48. Medeiros, A.; Pereira, E.; Moreira, A. *Notícia Explicativa Da Folha 9-D Penafiel Da Carta Geológica de Portugal à Escala 1:50 000 [Geologic Map at Scale 1:50 000 Sheet 9D Penafiel]*; Serviços Geológicos de Portugal: Lisboa, Portugal, 1980.
49. APA Solos Contaminados—Guia Técnico, Valores de Referência Para o Solo [Contaminated Soils—Technical Guide, Soil Reference Values]; Agência Portuguesa do Ambiente: Lisbon, Portugal, 2019.
50. Taylor, S.R.; McLennan, S.M. The Geochemical Evolution of the Continental Crust. *Rev. Geophys.* **1995**, *33*, 241. [[CrossRef](#)]
51. Medgold Resources Corp. *6º Relatório Semestral Relativo Ao 1º Semestre de 2016—Contrato de Prospecção e Pesquisa MN/PP/015/13 Valongo [6th Semester Report Relative to the 1st Semester of 2016—Exploration Contract MN/PP/015/13 Valongo]*; Medgold Resources Corp: Porto, Portugal, 2016.
52. Medgold Resources Corp. *5º Relatório Semestral Relativo Ao 2º Semestre de 2015—Contrato de Prospecção e Pesquisa MN/PP/015/13 Valongo [5th Semester Report Relative to the 2nd Semester of 2015—Exploration Contract MN/PP/015/13 Valongo]*; Medgold Resources Corp: Porto, Portugal, 2016.
53. Da Silva, E.B.; Gao, P.; Xu, M.; Guan, D.; Tang, X.; Ma, L.Q. Background Concentrations of Trace Metals As, Ba, Cd, Co, Cu, Ni, Pb, Se, and Zn in 214 Florida Urban Soils: Different Cities and Land Uses. *Environ. Pollut.* **2020**, *264*, 114737. [[CrossRef](#)]
54. Nogueira, T.A.R.; Abreu-Junior, C.H.; Alleoni, L.R.F.; He, Z.; Soares, M.R.; dos Santos Vieira, C.; Lessa, L.G.F.; Capra, G.F. Background Concentrations and Quality Reference Values for Some Potentially Toxic Elements in Soils of São Paulo State, Brazil. *J. Environ. Manag.* **2018**, *221*, 10–19. [[CrossRef](#)] [[PubMed](#)]
55. Sun, Y.; Li, H.; Guo, G.; Semple, K.T.; Jones, K.C. Soil Contamination in China: Current Priorities, Defining Background Levels and Standards for Heavy Metals. *J. Environ. Manag.* **2019**, *251*, 109512. [[CrossRef](#)] [[PubMed](#)]
56. Cabrera, F.; Clemente, L.; Díaz Barrientos, E.; López, R.; Murillo, J.M. Heavy Metal Pollution of Soils Affected by the Guadamar Toxic Flood. *Sci. Total Environ.* **1999**, *242*, 117–129. [[CrossRef](#)] [[PubMed](#)]
57. Ji, Y.; Feng, Y.; Wu, J.; Zhu, T.; Bai, Z.; Duan, C. Using Geoaccumulation Index to Study Source Profiles of Soil Dust in China. *J. Environ. Sci.* **2008**, *20*, 571–578. [[CrossRef](#)]
58. Pereira, E.; Cabral, J.; Cramez, P.; Moreira, A.; Noronha, F.; Oliveira, J.M.; Farinha Ramos, J.M.; Reis, M.L.; Ribeiro, A.; Ribeiro, M.L.; et al. *Carta Geológica de Portugal, Escala 1/200 000, Notícia Explicativa Da Folha 1 [Geologic Map of Portugal at Scale 1/200,000—Sheet 1]*; Serviços Geológicos de Portugal: Amadora, Portugal, 1992.
59. Wang, N.; Wang, A.; Kong, L.; He, M. Calculation and Application of Sb Toxicity Coefficient for Potential Ecological Risk Assessment. *Sci. Total Environ.* **2018**, *610–611*, 167–174. [[CrossRef](#)]
60. Sun, L.; Guo, D.; Liu, K.; Meng, H.; Zheng, Y.; Yuan, F.; Zhu, G. Levels, Sources, and Spatial Distribution of Heavy Metals in Soils from a Typical Coal Industrial City of Tangshan, China. *Catena* **2019**, *175*, 101–109. [[CrossRef](#)]
61. Xiao, H.; Shahab, A.; Li, J.; Xi, B.; Sun, X.; He, H.; Yu, G. Distribution, Ecological Risk Assessment and Source Identification of Heavy Metals in Surface Sediments of Huixian Karst Wetland, China. *Ecotoxicol. Environ. Saf.* **2019**, *185*, 109700. [[CrossRef](#)]
62. ESRI. *ArcGIS Pro 3.0.3*; [Computer Software]; ESRI: Redlands, CA, USA, 2021.
63. USEPA. *Supplemental Guidance for Developing Soil Screening Levels for Superfund Sites [R]*; Office of Solid Waste and Emergency Response: Washington, DC, USA, 2001.
64. USEPA. *Child-Specific Exposure Factors Handbook (EPA-600-P-00e002B)*; USEPA: Washington, DC, USA, 2002.
65. Chen, H.; Teng, Y.; Lu, S.; Wang, Y.; Wang, J. Contamination Features and Health Risk of Soil Heavy Metals in China. *Sci. Total Environ.* **2015**, *512–513*, 143–153. [[CrossRef](#)]
66. Huang, C.-L.; Bao, L.-J.; Luo, P.; Wang, Z.-Y.; Li, S.-M.; Zeng, E.Y. Potential Health Risk for Residents around a Typical E-Waste Recycling Zone via Inhalation of Size-Fractionated Particle-Bound Heavy Metals. *J. Hazard. Mater.* **2016**, *317*, 449–456. [[CrossRef](#)]
67. Li, H.; Qian, X.; Hu, W.; Wang, Y.; Gao, H. Chemical Speciation and Human Health Risk of Trace Metals in Urban Street Dusts from a Metropolitan City, Nanjing, SE China. *Sci. Total Environ.* **2013**, *456–457*, 212–221. [[CrossRef](#)]
68. US Department of Energy. *RAIS: Risk Assessment Information System*; US Department of Energy: Washington, DC, USA, 2004.
69. Cao, L.; Appel, E.; Hu, S.; Yin, G.; Lin, H.; Rösler, W. Magnetic Response to Air Pollution Recorded by Soil and Dust-Loaded Leaves in a Changing Industrial Environment. *Atmos. Environ.* **2015**, *119*, 304–313. [[CrossRef](#)]
70. Inácio, M.; Pereira, V.; Pinto, M. The Soil Geochemical Atlas of Portugal: Overview and Applications. *J. Geochem. Explor.* **2008**, *98*, 22–33. [[CrossRef](#)]
71. *Canadian Environmental Quality Guidelines Canadian Soil Quality Guidelines for the Protection of Environmental and Human Health: Summary Tables*; Canadian Environmental Quality Guidelines: Winnipeg, MB, Canada, 2007.
72. Couto, H.; Roger, G.; Fonteilles, M. Présence de Sills de Roches Ignées Acides Dans La Mine Sb-Au de Ribeiro Da Serra, District Dúrico-Beirão, Nord Portugal. Implications Métallogéniques. *Comptes Rendus De L'académie Des Sci.—Ser. IIA—Earth Planet. Sci.* **1999**, *329*, 713–719. [[CrossRef](#)]

73. Carvalho, P.C.S.; Neiva, A.M.R.; Silva, M.M.V.G.; da Silva, E.A.F. Geochemical Comparison of Waters and Stream Sediments Close to Abandoned Sb-Au and As-Au Mining Areas, Northern Portugal. *Geochemistry* **2014**, *74*, 267–283. [[CrossRef](#)]
74. Parra, A.; Filipe, P.; Falé, P. *Sistema de Informação de Ocorrência e Recursos Minerais Portugueses—SIORMINP [Information System of Occurrence and Mineral Resources]*; Laboratório Nacional de Energia e Geologia: Lisboa, Portugal, 2002.
75. Keshavarzi, B.; Tazarvi, Z.; Rajabzadeh, M.A.; Najmeddin, A. Chemical Speciation, Human Health Risk Assessment and Pollution Level of Selected Heavy Metals in Urban Street Dust of Shiraz, Iran. *Atmos. Environ.* **2015**, *119*, 1–10. [[CrossRef](#)]
76. Ferreira-Baptista, L.; de Miguel, E. Geochemistry and Risk Assessment of Street Dust in Luanda, Angola: A Tropical Urban Environment. *Atmos. Environ.* **2005**, *39*, 4501–4512. [[CrossRef](#)]

Disclaimer/Publisher’s Note: The statements, opinions and data contained in all publications are solely those of the individual author(s) and contributor(s) and not of MDPI and/or the editor(s). MDPI and/or the editor(s) disclaim responsibility for any injury to people or property resulting from any ideas, methods, instructions or products referred to in the content.